

Facile preparation and bifunction imaging of Eu-doped GdPO₄ nanorods with MRI and cellular luminescence

Qijun Du^a, Zhongbing Huang^{a*}, Zhi Wu^a, Xianwei Meng^{b*}, Guangfu Yin^a, Fabao Gao^c,
Lei Wang^c

^a College of Materials Science and Engineering, Sichuan University, Chengdu, 610065,
People's Republic of China.

Email: zbhuang@scu.edu.cn; Fax: 86-28-85413003; Tel: 86-28-85413003

^b Laboratory of Controllable Preparation and Application of Nanomaterials, Center
for Micro/nanomaterials and Technology, Technical Institute of Physics and
Chemistry, Chinese Academy of Sciences, Beijing 100190, People's Republic of
China.

E-mail: mengxw@mail.ipc.ac.cn; Fax: +86-10-62554670; Tel: +86-10-82543521

^c Molecular Imaging Center, Department of Radiology, West China Hospital of Sichuan
University, Address: No.2, 4th Keyuan Road, Chengdu, 610093, China.

Experimental section

Reagents and Materials

All chemicals used in this work were analytical-grade reagents obtained without further purification. $\text{Gd}(\text{NO}_3)_3$ (99.99%) was purchased from Best Reagent. EuCl_3 (99.99%) was obtained from Shandong Yutai Qingda Fine Chemical Plant. NaH_2PO_4 was purchased from Chengdu Kelong Chemical Reagent Company. *Bombyx mori* silks were purchased commercially, and were hydrolyzed into SF peptides according to our previous work.^[1] Luria-Bertani (LB) medium and Dulbecco's Modified Eagle Medium (DMEM) used for cell cultures were purchased from Sigma-Aldrich and GIBCO (UK), respectively, and fibroblast cells (L929) and human liver carcinoma (Hep-G2) were purchased from Shanghai Institute of Biochemical and Cell Biology.

Characterization

Characterization of Eu-doped GdPO_4 NRs: The morphology of synthesized NRs was observed with scanning electron microscopy (SEM, JEOL-5900LV, 20 kV, Japan) and transmission electron microscopy (HRTEM, JEOL-2000, 200 kV, Japan). The elements analysis of the samples was conducted with the X-ray photoelectron spectroscopy (XPS, ESCALab220I-XL, British, VG Scientific). X-ray diffraction patterns (XRD) of the as-synthesized samples were analyzed with DX-1000 diffractometer (Dandong Fangyuan Instrument Co. Ltd, Cu $\text{K}\alpha$ radiation, $\lambda = 1.5418 \text{ \AA}$, 40 kV, 80 mA) with step size of 0.06° . Raman spectra were recorded by a Laser Raman Spectrometer (InVia, Renishaw) with excitation at 532 nm. Thermogravimetric (TG) and differential scanning calorimetry (DSC) were carried out with a TG/SDTA851^e analyzer of METTLER-TOLEDO Co. (Switzerland) at a heating rate of $5 \text{ }^\circ\text{C}\cdot\text{min}^{-1}$ in alumina sample holders with alumina as a reference sample in air. The magnetic property of samples was investigated by vibrating sample magnetometer (VSM, Lake shore-7400, USA) with a step size of 1.42 cm^{-1} . The photoluminescence (PL) properties were investigated using the F-7000 FL Spectrophotometer excitation at 395 nm. The luminescent photographs were taken with a KODAK DX7590 Zoom digital camera.

Fourier transform infrared (FT-IR) spectra were recorded by an IR-Prestige-21 spectrometer.

Cell tests and optical imaging of Eu-doped GdPO₄ NRs: MTT assays of the L929 cell line were used to evaluate the cyto-compatibility of Eu-doped GdPO₄ NRs. This method is based on the formation of dark red formazan by the metabolically active cells after their exposure to MTT (3-(4,5-dimethylthiazol-2-yl)-2,5-diphenyltetrazolium bromide). 100 µL of cells were added to 96-well plates (BD Biosciences) at an initial concentration of approximately 5×10^4 cells/mL. When the cells reached confluence, different concentrations of as-prepared NRs (25, 50, 100, and 200 µg/mL) were added into the culture wells, respectively, and cells were cultured at 37 °C for 1 – 5 d. Control cells were incubated in a NR-free medium. In order to obtain the results of MTT assay, L929 cells were first cultured in MTT-PBS solution at 37 °C for 4h on 96-well plates. Then, DMSO was added into wells after the medium was removed. In the experiment, pure cells without adding NRs were used as control group. The absorbance at 490 nm was measured with a Micro Plate Reader 3550 (Bio-Rad) after the incubating solution was removed. The cell viability (%) = optical density (OD) of the treated cells/OD of the untreated cells. All experiments were performed in triplicate (n=3).

In order to evaluate the luminescence imaging *in vitro*, Hep-G2 cells were cultured with Eu-doped GdPO₄ NRs (150 µg/mL) for 8 h in high glucose Dulbecco's modified Eagle's medium (DMEM) (GIBCO), supplemented with 10% FBS (Hyclone) at 37 °C in a humidified atmosphere of 5% CO₂, and cell number was determined by nuclei stained with Hoechst33342. After cells were fixed by 4% paraformaldehyde for 10 min, 0.1% Triton X-100 was added for 5 min to extract the cells, then 1% bovine serum albumin-PBS solution was added in order to decrease nonspecific background staining. Hoechst33342 was added and stewed for 10 min. Finally, cells were washed with enormous PBS and observed directly under Nikon fluorescence microscope (Nikon Eclipse Ti-S, CCD: Ri1).

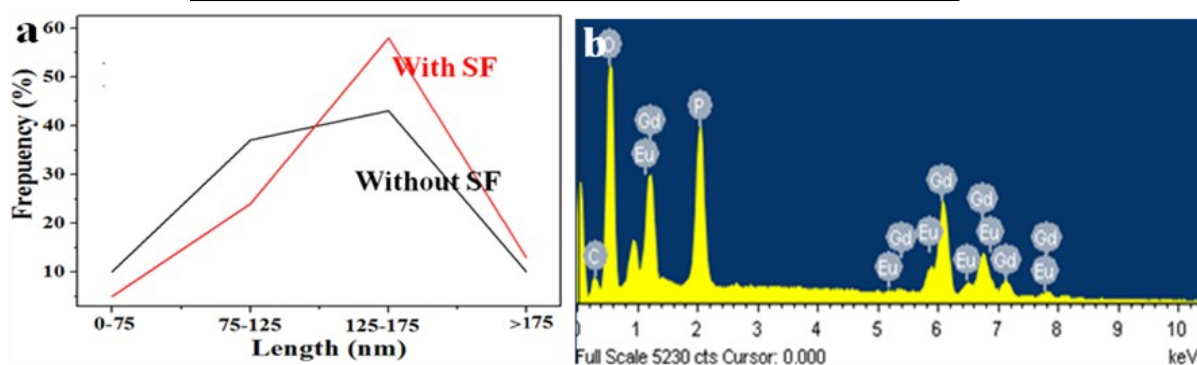
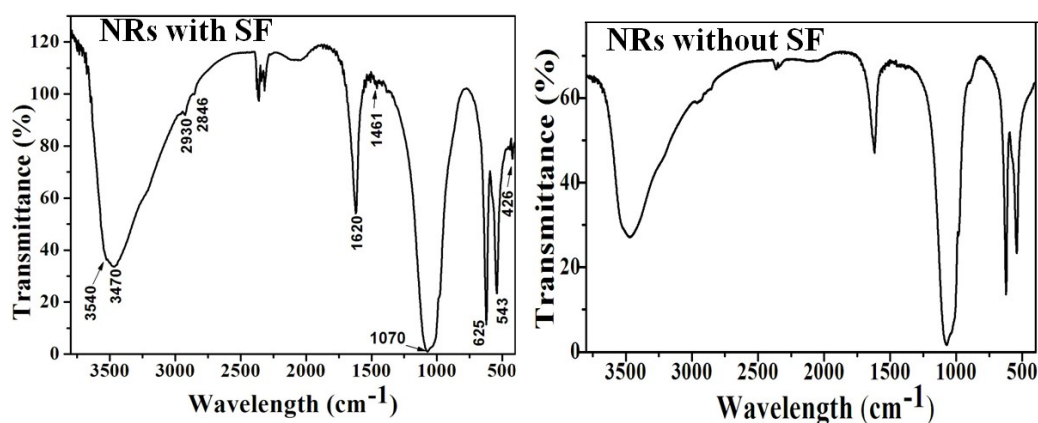
TEM was used to analyze the internalization of NRs in L929 cells. The medium was removed, and the L929 cells were washed 3 times with PBS. First, cells were

cultured at 37 °C for 3 d. Secondly, cells were collected in a centrifuge tube of 10 mL, then centrifuged for 10 min (1500 r/min) and washed 3 times with PBS. Thirdly, about 0.5% glutaraldehyde was added slowly along the centrifuge tube wall, cells were then kept for 30 min at 4 °C. Subsequently, cells were centrifuged for 15 min (13000 r/min), and then fixed with 3% glutaraldehyde, placed at 4 °C. Finally, re-fixation was carried out in 1 % osmium tetroxide. Then, dehydration was performed through ascending concentrations of acetone with three changes at 100%. Pure Epon-Araldite resin without methyl anhydride was added and infiltrated overnight at room temperature. The sample resin was polymerized for 18 h. The ultrathin sections of cells were obtained using a Leica Ultracut UCT ultramicrotome (MT-X; RMC Inc., Tucson, AZ). Thin sections (~60 nm) were post-stained with lead citrate, and observed and imaged in the transmission electron microscope (TEM, HITACHI-600 IV, 160 kV).

MR imaging and relaxation time measure were performed with a 7.0 T MR imaging system (BioSpec, Bruker, Germany). The prepared NRs were dispersed into agarose gel (0.5%) with different concentrations (0.25, 0.5, 1.0, 2.0 mM). Then these dispersions in 1.5 mL tubes were placed MRI system, respectively. T_1 -weighted images and T_1 values were obtained by the multi-slice multi-echo sequence. The measurement conditions were as follows: a field of view (FOV) of 4×4 cm, a slice thickness is 2.0 mm, the number of excitations (NEX) of 4, the size of the images of 256×256 , the value of repetition time (TR) of 180 ms, and echo time (TE) of 6.0 ms. Male mice (~30 g) were injected in the right axillary with 200 μ L cell suspension containing 4×10^6 A549 cell. The tumor usually appeared after tumor was transplanted for 14 d, and grew out about 500 mm³ within 20 d. Anesthesia was administered by gas before MR imaging. MR images were taken before and after 20 min of the intratumoral injection of Eu-doped GdPO₄ SF-NRs (50 μ L, 1 mg/mL, dispersed in saline). The T_1 signal intensity of a serial of MRI images of pre-injections (12 images) and post-injections (18 images) *in vivo* is measured with software Matlab 7.0. The experiments involving animals were performed in accordance with the guidelines of the Institutional Animal Care and Use Committee.

Table S1. Element Contents of Eu-doped GdPO₄ NRs (atomic %).

Element	NRs with SF	NRs without SF
C K	4.24	1.27
O K	75.76	76.02
P K	6.80	11.05
Eu K	0.86	1.27
Gd K	3.57	5.82
N K	8.77	4.57
Total	100.00	100.00
Eu/Gd	0.241	0.218

**Figure S1.** (a) Length distributions of Eu-doped NRs at different condition, (b) EDS spectrum of Gd_{0.8}Eu_{0.2}PO₄ NRs with SF attached to SEM.**Figure S2.** FT-IR spectra of Eu-doped NRs with/without SF.

The FT-IR spectrum of the synthesized sample is presented in Figure S2. The characteristic bands for PO₄³⁻ appear at 426, 543, 625, and 1070 cm⁻¹.^[2] The trace at 426 cm⁻¹ is attributed to the ν_2 bending vibration in PO₄³⁻, and the triply degenerated ν_4 bending vibrations are reflected as traces at 543 and 625 cm⁻¹, and the bands at 1070 cm⁻¹ to the ν_3 vibrations of PO₄³⁻ ions.^[3] The broad and high-intensity band extending from 2500 to 3600 cm⁻¹ derives from the ν_3 and ν_1 stretching modes of the hydrogen-

bonded H₂O molecules, and the band at 1620 cm⁻¹ derives from the ν_2 bending mode of the H₂O molecules. In this case, the band at 3540 cm⁻¹ arises from the stretching modes of the confined water, [4-6] and the smaller peaks at 2930 and 2847 cm⁻¹ are the asymmetric (ν_{as}) and symmetric (ν_s) stretching vibrations of C-H₂ of SF chains[7]; however, the peaks of 3540 cm⁻¹ and 2930 cm⁻¹ in the spectrum of NRs without SF are not obvious, indicating that there are lots of hydroxyl groups and a few of SF peptides in or on the Eu-doped GaPO₄ SF-NRs.

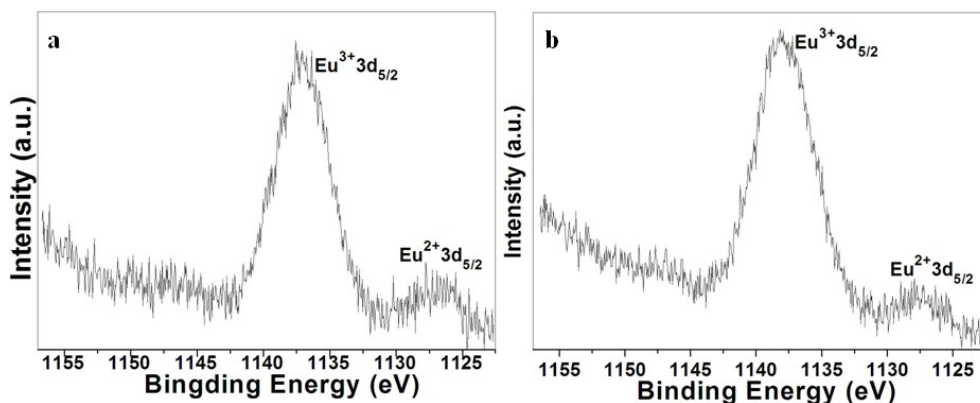


Figure S3. Eu high-resolution XPS spectra of the doped GdPO₄ NRs (a) with SF and (b) without SF.

To further investigate the chemical environment of two samples, high-resolution spectroscopy on Eu (3d) was performed. In Figure S3, the stronger peak at 1137 eV and the weaker peak at 1127 eV are attributed to Eu³⁺ 3d_{5/2} and Eu²⁺ 3d_{5/2}, respectively, and the peak area of Eu²⁺ in the pattern of SF-NRs (Figure S3a) is larger than that of NRs without SF (Figure S3b), suggesting that Eu²⁺ ions existed on the SF-NRs surface is more than that on the surface of the doped NRs without SF. The appearance of Eu²⁺ should result from the redox of tyrosine in SF peptides and the impure reagent of EuCl₃.

Eu-doped GdPO₄ NRs (1 mg/mL) in milliQ water were monitored by analyzing the evolution with aging time of their UV visible absorbance spectra (JASCO V-570 spectrophotometer). As shown in Figure S4, it can be found that Eu-doped GdPO₄ SF-NRs and NRs without SF almost exhibit the same absorption spectra. However, in milliQ water, sedimentation took place during at least 5 min. Compared to NRs without SF, the Eu-doped SF-NRs exhibit better dispersion in milliQ water.

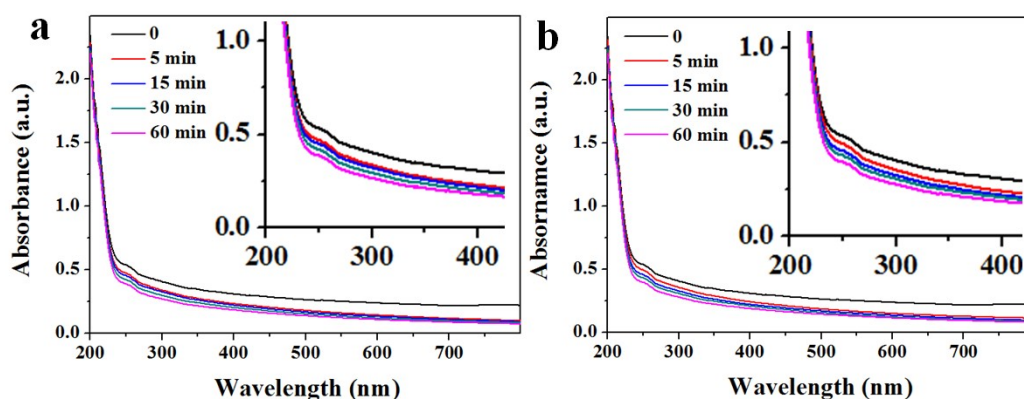


Figure S4. Evolution with aging time of the UV-visible absorption spectra recorded for Eu-doped GdPO₄ (a) without SF and (b) with SF dispersed in milliQ water (pH = 6.95). The inserts are amplification of their correspond image.

The influence of SF peptides on the formation of Eu-doped NRs is further investigated with TEM images shown in Figure S5 and S6. The size and shape of the nanomaterials can be tailored by adjusting reaction time. When no SF peptide was in the mixed solution, only short NRs of about 150 nm of length (Figure S5 and S6a) and nanoparticles of 20 nm diameter (shown by red arrows in Figure S5a) were obtained, all other reaction conditions were kept the same. When only SF peptides were added into the reaction solution, only shorter NRs with 150 nm of length in Figure S6a) were obtained under other same reaction conditions in 20 min. The lengths of NRs were increased to 50-200 in 50 min of reaction time (Figure S6b). However, when the reaction time was 80 min, longer NRs (Figure S6c) were obtained, compared with NRs without SF in Figure 5c. The result indicates that SF peptides can help to form the thinner NRs due to the hydrophobic and hydrophilic groups in SF peptides.

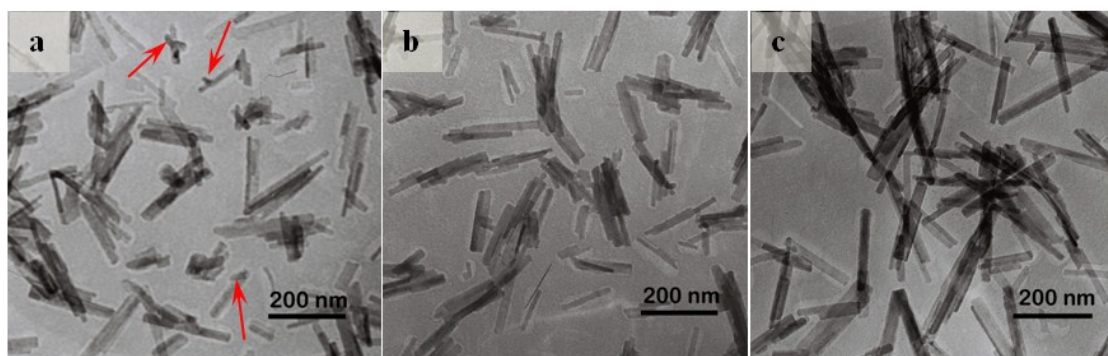


Figure S5. TEM images of doped NRs without SF at a different growth time: (a) 20 min, (b) 50 min, (c) 80 min, respectively.

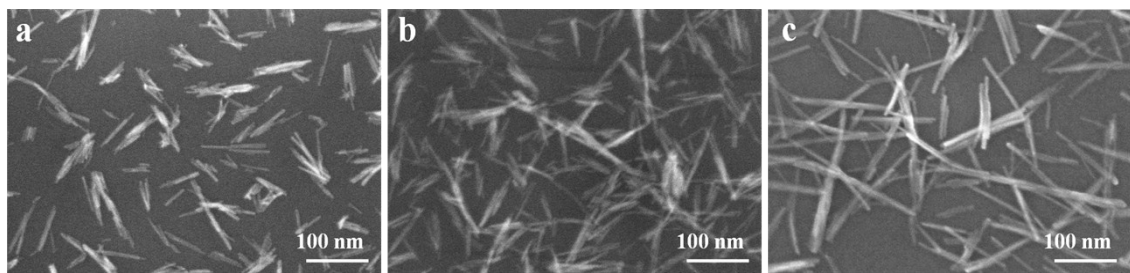


Figure S6. SEM images of doped NRs with SF at a different growth time: (a) 20 min, (b) 50 min, (c) 80 min, respectively, (d) length distributions of doped NRs at different growth times.

In order to evaluate the effect of SF coating on the degradation of NRs, the Eu-doped GdPO_4 NRs with/without SF are immersed in PBS (pH=7.2) for different time (Figure S7a). After NRs are immersed in PBS for 1–5d, the degradation ratio can be obtained by measuring the released Gd^{3+} concentrations from NRs into PBS and calculating the degraded amount of NRs. Samples of the released Gd^{3+} were prepared as following: first, NRs were dispersed in PBS (20 mL) and quantified into the different concentration of PBS solutions (0.20 mg/mL of NRs). After 1d, 3d and 5d, 1 mL solution samples were obtained from the above solutions, respectively. The concentrations of released Gd^{3+} were analyzed with inductively coupled plasma atomic emission spectrometer (ICP-AES, SPECTRO ARCOS, Germany). Then, these Gd^{3+} concentrations could be transferred into the amount of degraded NRs according to the $\text{Gd}_{0.8}\text{Eu}_{0.2}\text{PO}_4$ initial formula. Finally, the degradation ratio (%) = the amount of degraded NRs/the amount of NRs added into PBS. Moreover, 10 mg NRs were immersed in 10 mL FBS (fetal bovine serum, Chengdu hary biological engineering Co., LTD) at 37 °C. After 1, 3 and 5 days, 3 mL supernatants were collected, respectively. The supernatants were boiled in a digestion solution containing mixed acids (nitric acid: perchloric acid, v : v = 3 : 1) for 1 h. Gd^{3+} concentration was determined by ICP-AES. The degradation ratio (%) = the amount of degraded NRs/the amount of NRs added into FBS. As shown in Figure S7b, although the degradation ratios of NRs in FBS are obviously larger than those in PBS due to the catalysis of bio-enzymes in serum, SF peptides on SF-NRs could slow significantly the release of metal ions in 1 day, and also slow slightly their release in 3 – 5 days, avoiding the higher concentration accumulation of excessive metal ions inside cell and apoptosis of cells.

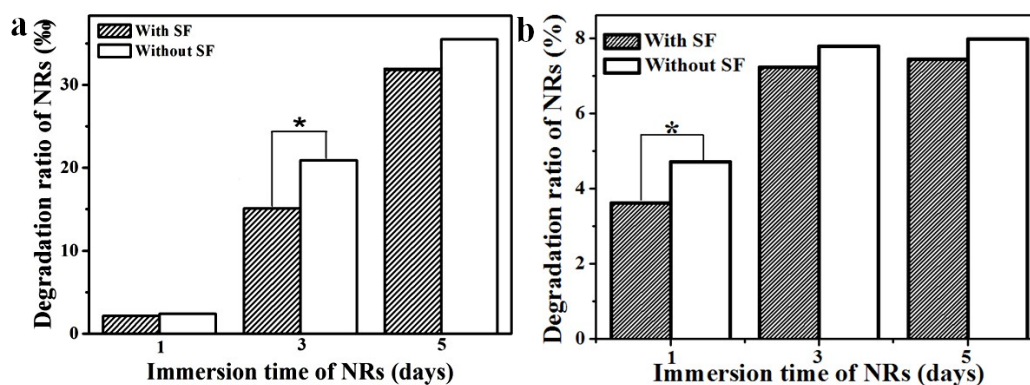


Figure S7. The ratio of degradation of Eu-doped GdPO₄ NRs with/without SF after the immersion for 1–5 d in PBS (a) and FBS (b). (* represents significant difference between two corresponding group, $p < 0.05$).

As shown in Figure S8, the morphology of L929 cells could be obtained after co-incubation with the prepared NRs suspension with the different concentrations (0, 25, 50, 100 and 200 $\mu\text{g}/\text{mL}$) for 1 d. The pictures in Figure S8b–e show that many cells contacted with NRs. At the lower concentrations (25 and 50 $\mu\text{g}/\text{mL}$), more cells were could be clearly observed. The treatments of NRs without SF of a higher concentration (100 and 200 $\mu\text{g}/\text{mL}$) produced a great deal of extra material deposited on the cells and “mechanically” induced extra stress to damage the cells. The results suggest that the Eu-doped GdPO₄ NRs with SF show a lower cyto-toxicity.

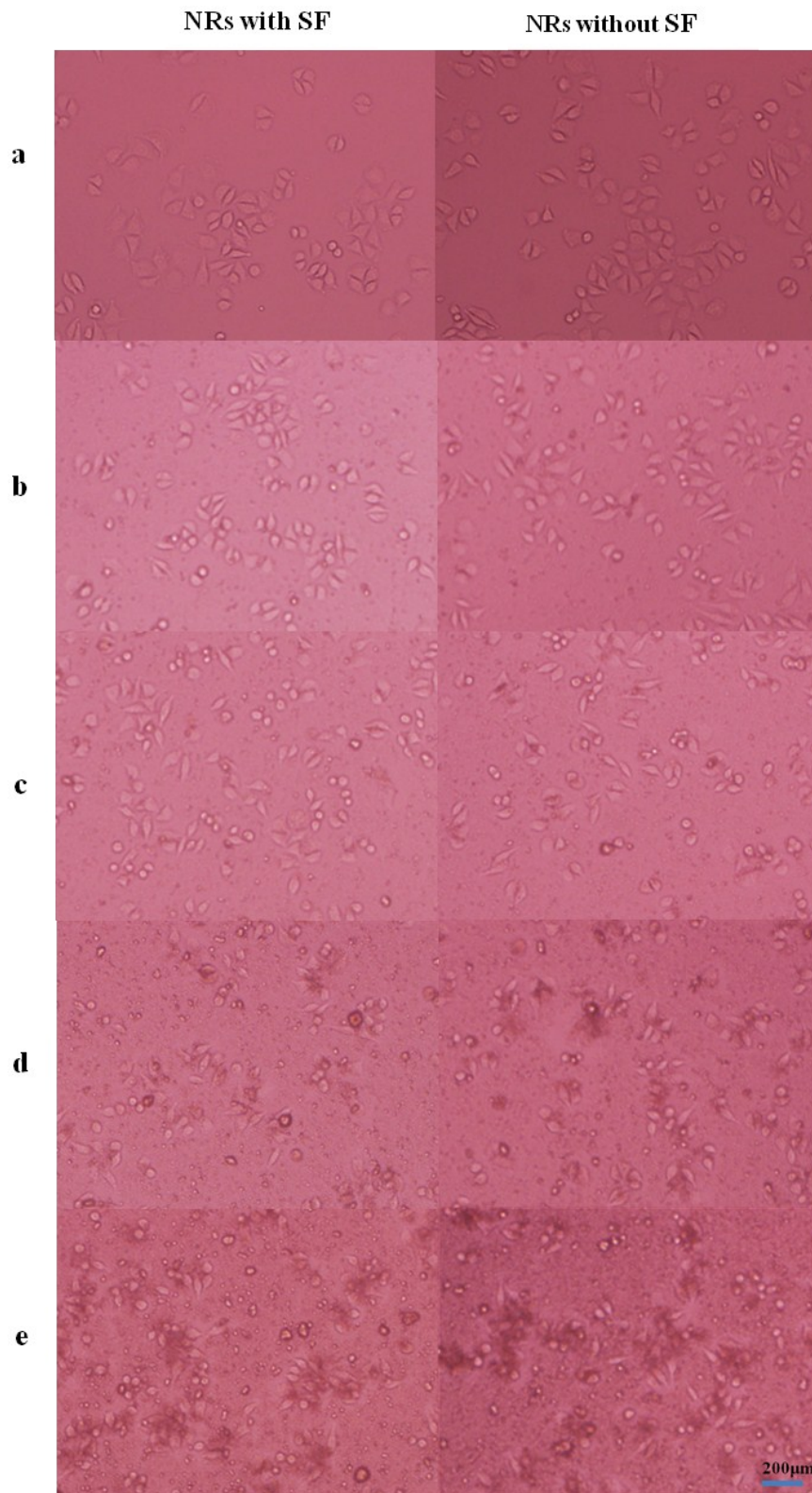


Figure S8. Photomicrographs of L929 cells cultured after 1 day at different concentrations of NRs: (a) 0 µg/mL; (b) 25 µg/mL, (c) 50 µg/mL, (d) 100 µg/mL and (e) 200 µg/mL.

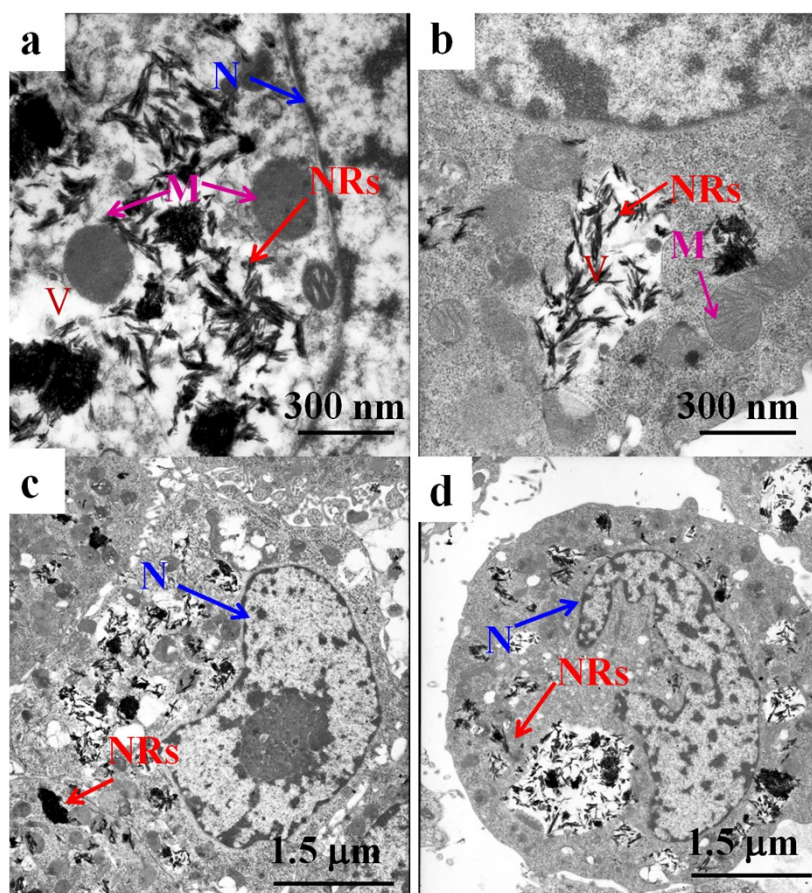


Figure S9. TEM images of thin sections of L929 cells co-cultured for 3d with 100 µg/mL NRs: (a,c) without SF, (b,d) with SF. (N is nucleus, M is mitochondrion, V is vacuoles).

With seven unpaired 4f electrons ($^8S_{7/2}$), the Gd^{3+} ion, which can produce a large electron magnetic moment, is one of the best metal ions for positive MR imaging.^[8-10] Gd^{3+} ions possess a large number of unpaired electrons, and Gd^{3+} -based nanoparticles have the potential to be used as contrast agent for T_1 -enhanced MR imaging. Specially, paramagnetic gadolinium chelates (such as Gd-diethylenetriaminepentaacetic acid, Gd-DTPA) are clinically used as T_1 -weighted agents, providing a positive contrast.^[11-13] Furthermore, we also studied their luminescent properties due to Eu ions doping. Figure S10a and b show that luminescence photographs of the as-obtained Eu-doped $GdPO_4$ NRs exhibit red emission under violet light excitation at 395 nm, which are consistent with the results of emission spectra (Figure S11).

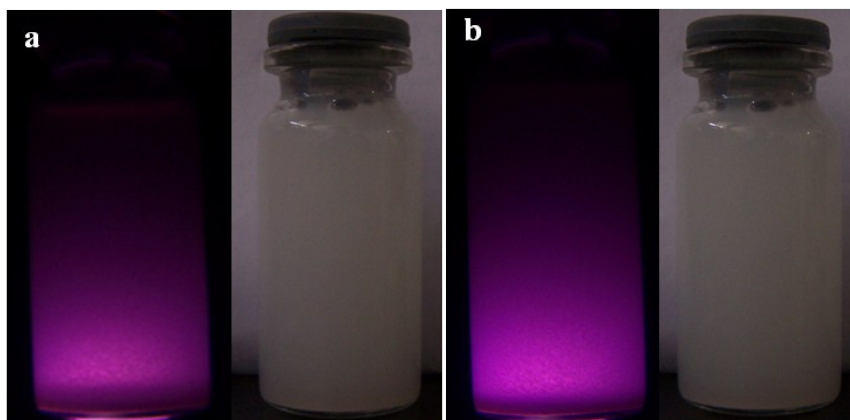


Figure S10. Luminescent images and corresponding bright images of Eu-doped GdPO_4 NRs: (a) without SF; (b) with SF, which are dispersed in distilled water.

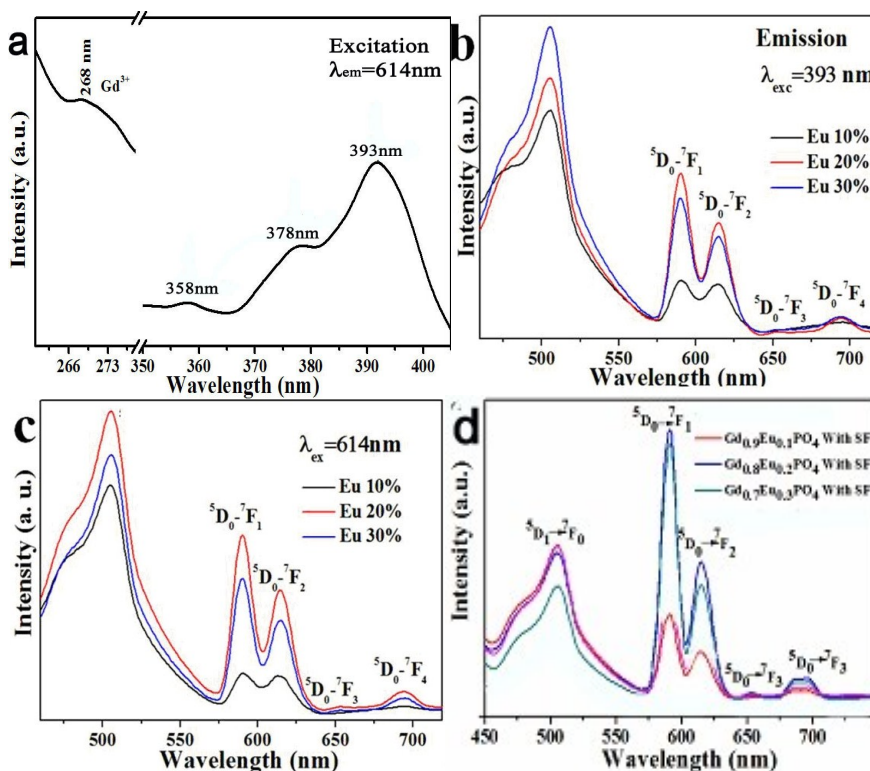


Figure S11. Excitation spectrum (a) and Emission spectra of the prepared Eu-doped GdPO_4 NRs in different condition: (b) without SF; (c) with SF; (d) doped NRs with SF calcined at 600°C for 3 h.

Figure S11a shows the excitation spectrum of the $\text{Eu}_{0.2}\text{Gd}_{0.8}\text{PO}_4$ (20% Eu content in the reactive metal ions) SF-NRs monitored at the most intense Eu^{3+} emission band (618 nm). The broad excitation bands centered at 393, 378 and 358 nm are observed, which have been previously observed for several Eu-doped LnPO_4 systems and attributed to the f-f transitions Eu^{3+} and the excitation of an electron of neighboring O^{2-} from the top of the valence band to the lowest unoccupied 4f levels of the doped Eu^{3+} . A

weak and broad excitation band of about 268 nm is attributed to the absorption of Gd^{3+} . The Figure S11b and c show the emission spectra of Eu-doped $GdPO_4$ samples without and with SF, respectively, which are obtained at the different Eu content in the reactive metal ions. Since the 4f-5d transitions are electric-dipole allowed, the absorption and emission of Eu^{2+} ions are characterized as efficient broad bands in many hosts. Upon the excitation of ~ 395 nm, it is observed that the PL spectrum consists of a single green emitting broad band with a maximum at 509 nm, which is ascribed to the electric-dipole allowed 4f-5d transition of the Eu^{2+} ions. The peaks at 591, 613 and 695 nm should correspond to ${}^5D_0 \rightarrow {}^7F_{1,2,4}$ transitions of Eu^{3+} due to efficient energy transfer from Gd^{3+} to Eu^{3+} . The most intense emission spectrum in Figure S11c is from $Gd_{0.8}Eu_{0.2}PO_4$ SF-NRs, and the stronger red luminescence could be observed in the image of Figure S10b, further suggesting that more Eu^{3+} ions are doped to enter onto/into NRs in the help of SF peptides. Figure S11d shows the stronger emission spectra of Eu-doped $GdPO_4$ NRs calcined at $600^\circ C$ for 3 h, compared with those of NRs before calcination, indicating that some water molecules confined in the pores of Eu-doped NRs can quench the luminescence intensity of Eu^{3+} , and the calcination could obviously decrease the quenching effect of water molecules in the as-prepared NR.^[18]

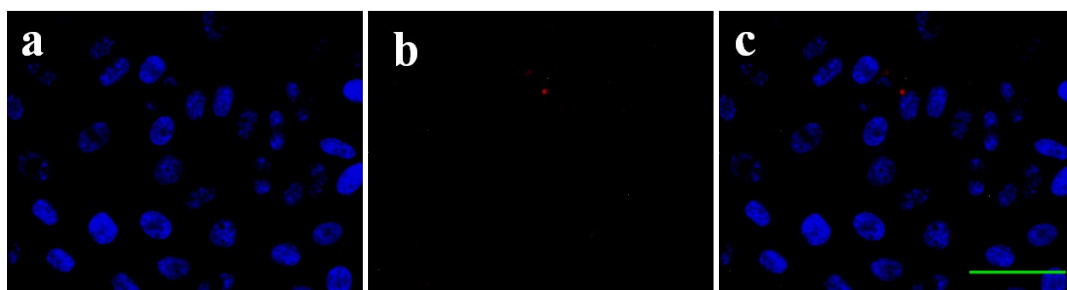


Figure S12. The dark (a, b) and overlapped background images under violet excitation (c) of HepG2 cells with Eu-doped $GdPO_4$ NRs without SF, and the bar is 50 μm .

References:

1. B. Abécassis, F. Lerouge, F. Bouquet, S. Kachbi, M. Monteil and P. Davidson, *J. Phys. Chem. B*, 2012, **116**, 7590.
2. K. C. Blakeslee and R. A. Condrate, *J. Am. Ceram. Soc.*, 1971, **54**, 559.
3. M. Marković, B. O. Flower and M. S. Tung, *J. Res. Natl. Inst. Stand. Technol.*, **2004**, **109**, 553.
4. S. H. Cho, S. M. Joo, J. S. Cho, J. K.

- Lee and H. Kim, *J. Ceram. Process. Res.*, 2004, **6**, 57.
5. B. Chen and C. Liang, *Ceram. Int.*, 2007, **33**, 701.
 6. R. S. Ningthoujam, *Pramana – J. Phys.*, 2013, **80**, 1055.
 7. M. Deng, Z. Huang, Y. Zou, G. Yin, J. Liu and J. Gu, *Colloid. Surf. B: Biointerf.*, 2014, **116**, 465.
 8. W. Lin, T. Hyeon, G. M. Lanza, M. Zhang and T. J. Meade, *MRS Bull.*, 2011, **34**, 441.
 9. H. B. Na, I. C. Song and T. Hyeon, *Adv. Mater.*, 2009, **21**, 2133.
 10. J. Y. Park, E. S. Choi, M. J. Baek, G. H. Lee, S. Woo and Y. Chang, *Eur. J. Inorg. Chem.*, 2009, 2477.
 11. N. Sakai, L. Zhu, A. Kurokawa, H. Takeuchi, S. Yano, T. Yanoh, N. Wada, S. Taira, Y. Hosokai, A. Usui, Y. Machida, H. Saito and Y. Ichiyangi, *J. Phys.: Conf. Ser.*, 2012, **352**, 012008.
 12. J. Y. Park, M. J. Baek, E. S. Choi, S. Woo, J. H. Kim, T. J. Kim, J. C. Jung, K. S. Chae, Y. Chang and G. H. Lee, *ACS Nano*, 2009, **3**, 3663.
 13. M. Ahrén, L. Selegård, A. Klasson, F. Söderlind, N. Abrikossova, C. Skoglund, T. Bengtsson, M. Engström, P.-O. Käll and K. Uvdal, *Langmuir*, 2010, **26**, 5753.
 14. B. Mutelet, S. Boudin, O. Pérez, J. M. Rueff, C. Labbé and P. A. Jaffrès, *Dalton Trans.*, 2015, **44**, 1186.
 15. H. Zhou, Y. Jin, M. Jiang, Q. Wang and X. Jiang, *Dalton Trans.*, 2015, **44**, 1102.
 16. X. Wang, C. Liu, T. Yu and X. Yan, *Phys. Chem. Chem. Phys.*, 2014, **16**, 13440.
 17. F. Chen, P. Huang, C. Qi, B. Lu, X. Zhao, C. Li, J. Wu, D. Cui and Y. Zhu, *J. Mater. Chem. B*, 2014, **2**, 7132.
 - 18 a) M. N. Luwang, R. S. Ningthoujam, Jagannath, S. K. Srivastava and R. K. Vatsa, *J. Am. Chem. Soc.*, 2010, **132**, 2759. b) M. N. Luwang, R. S. Ningthoujam, S. K. Srivastava and R. K. Vatsa, *J. Am. Chem. Soc.* 2011, **133**, 2998. c) R. S. Ningthoujam, *Pramana – J. Phys.*, 2013, **80**, 1055.